

# Tri-layer Scaffold with Cardiosphere-Derived Cells for Heart Valve Tissue Engineering

Qi Chen <sup>a,b,\*</sup>, Arne Bruyneel <sup>c</sup>, Carolyn Carr <sup>d</sup>, Jan Czernuszka <sup>b</sup>

<sup>a</sup> R&D.cn, Guangzhou International Bio-Island, Guangzhou, 510005, China

<sup>b</sup> Department of Materials, University of Oxford, Oxford, OX1 3PH, UK

<sup>c</sup> Cardiovascular Institute, Stanford University, Stanford, CA 94305, USA

<sup>d</sup> Department of Physiology, Anatomy and Genetics, University of Oxford, Oxford, OX1 3PT, UK

\* Corresponding author. Tel.: +86 13611635050; E-mail address: chenqimike@gmail.com

## Abstract

Natural polymers collagen, glycosaminoglycans, and elastin are promising candidate materials for heart valve tissue engineering scaffolds. This work produced tri-layer scaffolds that resembled the layered structures of the extracellular matrices of native heart valves. The scaffolds showed anisotropic bending moduli (in both dry and hydrated statuses) depending on the loading directions (lower in the With Curvature direction than in the Against Curvature direction), which mimicked the characteristic behaviour of the native heart valves. The interactions between cardiosphere-derived cells and the scaffolds were characterized by multi-photon microscopy, and relatively similar cell distributions were observed on different layers (a cell density of 3000~4000 mm<sup>-3</sup> and a migration depth of 0.3~0.4mm). The tri-layer scaffold has represented a forwarding step from the previous studies, in attempting to better replicate a native heart valve structurally, mechanically, and biologically.

## 1. Introduction

Heart valves are very important cardiac organs as they ensure the unidirectional blood flow through the heart. Heart valve diseases are a major health issue and are significant causes of mortality worldwide [1]. Tissue engineered heart valve (TEHV) is believed to be a promising candidate for a long-lasting and curative heart valve replacement [2], which has the potential to provide a solution to the heart valve diseases.

In a TEHV, the scaffold provides dimensional support and living environment for the cells, and thus is one of the essential elements. Decellularized heart valve tissues have maximally respected the complexity and integrity of the extracellular matrices (ECM) in native heart valves [3] (e.g. the layered structures of fibrosa, spongiosa, and ventricularis), and could be a good option for TEHV scaffolds. There are, however, issues related to the decellularized scaffolds: for scaffolds from xenograft tissues, immunological rejection might still occur despite even near-complete decellularization [4], and for scaffolds from allograft tissues, the availability of donor valves is still very limited [2]. Synthetic polymer scaffolds have the advantages of greater reproducibility, fewer immunogenic reactions, and unlimited supply over the decellularized scaffolds [5]. Efforts have also been made to create synthetic polymer scaffolds with layered structures mimicking native heart valves [6]. Yet limitations still exist such as lack of endothelialization, valve construct dilation and regurgitation, and potential toxicity of the degradation products [5, 7, 8].

The possibility of using natural ECM constituents (collagen, glycosaminoglycans, and elastin) of the native heart valves to fabricate scaffolds has therefore been investigated [9, 10]. The natural polymers could provide a solution to the less controllable and repeatable decellularization process; and given their intrinsic bioactivities, the natural polymers could also better facilitate the remodeling of the engineered tissues compared with the synthetic polymers. We have previously examined a bi-layer scaffold comprising a collagen-rich layer and an elastin-rich layer, which represented the fibrosa and ventricularis respectively [11]. This paper will present a tri-layer scaffold that is one step further towards mimicking the layered structures of a native heart valve.

Mechanically, this scaffold will try to copy the characteristic anisotropic bending behaviour of the native heart valve, i.e. it is easier to bend towards the ventricularis side, referred as 'With Curvature' (WC), than towards the fibrosa side, referred as "Against Curvature" (AC), as shown in Fig 1.

A TEHV also needs to maintain its viability both in vitro and in vivo, which requires another essential element - cells. So far, the two major categories of

candidate cells for TEHVs are the cardiovascular-derived cells and the stem cells, due to either high cardiac tissue commitment, or easy availability and high differentiation capabilities [13]. A relatively newly discovered type of cardiac progenitor cells, cardiosphere-derived cells (CDCs) [14] may potentially enjoy the combined advantages of the two categories of candidate cells. This study, therefore, applies CDCs to the tri-layer scaffolds, and assesses the scaffolds' biocompatibility in addition to their mechanical properties.

## 2. Materials and Methods

### 2.1 Scaffold Fabrication

Type I collagen (from bovine Achilles tendon, Sigma-Aldrich Ltd, UK), chondroitin-4-sulfate (C4S, sodium salt, from bovine trachea, Sigma-Aldrich Ltd, UK) and elastin (from bovine neck ligament, Sigma-Aldrich Ltd, UK), were selected as scaffold materials.

The scaffold materials were all firstly made into suspensions with various compositions designed for respective layers: 100%collagen for fibrosa, 50%collagen-50%C4S for spongiosa, and 20%collagen-80%elastin for ventricularis. All suspensions had a concentration of 1% wt/v.

100%collagen and 20%collagen-80%elastin suspensions were made with 0.05 M acetic acid (pH 3.2) [15, 16]. For 50%collagen-50%C4S suspension, the collagen was firstly suspended in the same acetic acid. Then the C4S was added into the suspension, instantly co-precipitating with collagen and forming agglomerates. The agglomeration was reduced by drop-wise adding 2M sodium hydroxide solutions to the suspension until the pH value reached 7 [17], resulting in a homogeneous suspension of fine collagen-C4S co-precipitates.

After being made, the suspensions were subjected to a vacuum of 10kPa for 1 hour at room temperature to remove the entrapped air bubbles. The de-gassed suspensions were then cast into polytetrafluoroethylene (PTFE) molds and frozen at -20°C (EU7120C, Electrolux, UK). For single-composition scaffolds, molds were disc-shaped, 12.5mm in diameter, and 1.5mm in thickness. For tri-layer scaffolds, molds had dimensions of 40×12×5 mm<sup>3</sup> and multiple cast-freeze procedures were performed to achieve layered structures. The 100%collagen layer was firstly cast and frozen, followed by the 50%collagen-50%C4S layer and the 20%collagen-80%elastin layer. The volume of the suspension for each casting was controlled so as to give an equal thickness to each layer. The frozen suspensions were all freeze-dried in a Christ I-5 freeze-dryer (Martin Christ Gefriertrocknungsanlagen GmbH, Germany) for 24

hours under a vacuum of 5Pa, to achieve the porous solid scaffolds.

## **2.2 Scanning Electron Microscopy**

The morphology of the tri-layer scaffolds was characterized by a scanning electron microscope (SEM, JSM840F, JEOL Ltd, Japan) with an accelerating voltage of 4kV. One representative scaffold was sectioned with a sharp razor blade, and the cross-section was examined.

## **2.3 Mechanical Tests on Dry Scaffolds**

Unidirectional three-point bend tests were conducted using a DMA7 (PerkinElmer, MA) on dry tri-layer scaffolds at room temperature. The 40×12×5 mm<sup>3</sup> samples were loaded at a cross-head speed of approximately 0.5mm/min with a span of 20mm. The tests were conducted in both WC direction (sample bent towards the collagen-elastin layer) and AC direction (sample bent towards the collagen layer). Six samples of each group were tested.

## **2.4 Mechanical Tests on Hydrated Scaffolds**

Mechanical tests were also conducted on hydrated tri-layer scaffolds, which were in a state more similar to that in vivo. The extremely low load and high sensitivity needed made three-point bend tests on the hydrated scaffolds practically infeasible. Therefore, a “self-deflection” test was designed to give an easier approach to measure the mechanical properties of the hydrated scaffolds.

The self-deflection tests were carried out as shown in Fig 2. The hydrated tri-layer scaffolds (having been immersed in 0.1M phosphate buffered saline at room temperature for 1 hour) were clamped with a span of 20mm, and were allowed to self-deflect, with the weight of the PBS absorbed by the scaffolds as the load. The tests were also performed in both WC and AC directions. The deflections were recorded by a camera (450D, 50mm, F1.8, Canon, Japan) and measured by ImageJ (National Institutes of Health, USA). Six samples of each group were tested.

## **2.5 Cell Harvest and Isolation**

Cardiosphere-derived cells (CDCs) were isolated from adult Sprague Dawley rats

(Harlan Laboratories, UK) and were expanded in accordance with published protocols [18-20]. Briefly, explanted rat hearts were minced into small explant pieces, plated on fibronectin-coated petri dishes with complete explant medium (CEM), and then incubated at 37°C with 5% CO<sub>2</sub>. After approximately one week, cells that had grown out from the explants were isolated and re-plated in poly-d-lysine-coated 24-well plates with cardiosphere growth medium (CGM). Cardiospheres formed after 2–3 days. They were subsequently harvested by mechanical trituration and plated in CEM in fibronectin-coated flasks to culture for CDCs.

## 2.6 Cell Culture

For cell culture, the original 40×12×5 mm<sup>3</sup> tri-layer scaffolds were sectioned into 1.5×12×5 mm<sup>3</sup> pieces and seeded with CDCs as shown in Fig 3. Before cell seeding, the scaffolds (6 samples) were sterilized by three 30-minute washes with 100% ethanol, followed by three 30-minute washes with Dulbecco's phosphate buffered saline (DPBS). Then they were placed in fibronectin-coated 24-well plates and immersed in CEM. CDCs (50000 cells per scaffold) were seeded onto the scaffolds and cultured for 7 days at 37°C with 5% CO<sub>2</sub>. For comparison purposes, CDCs were also cultured on the disc-shaped single-composition scaffolds (6 samples of each group) using the same method.

## 2.7 Multi-photon Microscopy

Multi-photon microscopy (MPM) is a non-invasive method of fluorescence imaging, most suitable for biological samples [21], and was therefore used to characterize the distribution and migration of cells on the scaffolds. Collagen and elastin were auto-fluorescent by second-harmonic generation (SHG) and two-photon excitation (TPE) respectively [22]. The cells were stained with rhodamine phalloidin (Life Technologies Ltd, UK) to be fluorescent.

The scaffolds (one representative sample from each group) were imaged by a modified BioRad Radiance 2100MP Multi-photon Microscope (Zeiss, Germany). Excitation beam had a wavelength of 800 nm. The signals from collagen, elastin and cells were collected with 390nm, 525nm, and 595nm band-pass filters, and were shown blue, green and red respectively on the images [23].

For each image, a Z stack consisting of multiple slides was firstly taken, from the top surface of the scaffold to the deepest level in the scaffold where signals from cells could still be detected. The slides of the Z stacks were then reconstructed by

ImageJ (National Institutes of Health, USA) into 2-D projections in the Z direction. Specifically for the tri-layer scaffold, the 2-D projections were further connected by Panorama Tools (University of Applied Sciences Furtwangen, Germany) to form a panorama across the sample (see Fig 4). The cells on the images were counted by ImageJ. With the volumes of the Z stacks known (from the frame sizes and the stack depths), the cell densities could then be calculated.

### 3. Results

#### 3.1 Scanning Electron Microscopy

The layered scaffolds were successfully fabricated with the cast-freeze procedures. Fig 5 shows the cross-section micrograph of the tri-layer scaffold. It exhibited distinct layered structures with well-connected interfaces.

#### 3.2 Mechanical Properties

Fig 6 presents the representative load-deflection curves showing the bending anisotropy of the tri-layer scaffolds. The  $E_{\text{bend1}}$  and  $E_{\text{bend2}}$  were calculated from the slopes on the curves with the following equation, and were listed in Table 1.

$$E_{\text{bend}} = \left(\frac{\delta P}{\delta D}\right) \frac{l^3}{48I} \quad \text{Eq.1}$$

In Eq.1,  $\delta P/\delta D$  is the slope of the load-deflection curve with P being the load and D being the deflection, l is the span distance, and I is the second moment of area (l and I remaining constant during the test).

We could see that, in dry status, the tri-layer scaffolds had similar  $E_{\text{bend1}}$  values in the WC and AC directions, and had higher  $E_{\text{bend2}}$  values in the AC direction. The different  $E_{\text{bend2}}$  values led to different eventual deflections under the same load, i.e. the bending anisotropy.

Fig 7 shows a self-deflected tri-layer scaffold in hydrated status, whose deflection (D) is determined by Eq.2

$$D = h - \frac{t}{2} \quad \text{Eq.2}$$

where t is the thickness of the scaffold, and h is the distance between the central position of the clamps (i.e. the initial central position of the scaffold) and the lower surface of the deflected scaffold.

It could be seen that the bending anisotropy of the tri-layer scaffold was well

maintained in the hydrated status, i.e. there was a larger deflection in the WC direction than in the AC direction (see Table 2).

### 3.3 Scaffold Shrinkage During Cell Culture

After 7 days' culture, certain extents of shrinkage occurred on the single-composition scaffolds (see Fig 8). Scaffold shrinkage in the radial direction was measured from Fig 8 and correspondent area reduction was listed in Table 3. It could be seen that the shrinkage was much more prominent on the collagen-elastin scaffolds than on the other two types of scaffolds.

### 3.4 Multi-photon Microscopy

Fig 9 shows the MPM images of the single-composition scaffolds. Table 4 lists the depths and volumes of the Z stacks for those images, as well as the number of cells and the cell densities in the given stacks. The stack depth was smaller on the collagen-elastin scaffolds and was larger on the collagen-C4S scaffolds, indicating different cell migration behaviours. A much higher cell density was also observed on collagen-elastin scaffolds.

Fig 10 and Table 5 demonstrate the cell distribution on the tri-layer scaffold. It could be seen that the cells distributed relatively evenly on all three layers, with the collagen-C4S layer having a slightly larger stack depth and a slightly lower cell density. Shrinkage on tri-layer scaffold could also be seen when we compared the thickness of layers in Fig 10 with that in Fig 5 ( $\sim 700\mu\text{m}$  vs  $\sim 1400\mu\text{m}$ ), although the proportion of each layer still remained approximately equal in Fig 10, indicating similar degrees of shrinkage on all three layers after cell culture.

## 4. Discussion

The layered structures are one of the most important features of the native heart valves. The cast-freeze procedure was able to produce integrate tri-layer scaffolds which mimicked the native heart valve ECM.

We have previously characterized the morphologies of single-composition scaffolds with the compositions corresponding to respective heart valve layers, as well as the morphologies of bi-layer scaffolds [10, 11]. Compared with the single-composition and the bilayer scaffolds, the tri-layer scaffold exhibits a

lower degree of homogeneity in the pore structures, especially within the collagen-C4S layer. This is likely to have been caused by the process of casting the collagen-elastin layer onto the frozen collagen-C4S layer in the multiple cast-freeze procedure. Since the frozen suspensions were briefly left under room temperature for a better inter-layer connection, the crystals in the frozen collagen-C4S layer might have partially melted due to the lower melting point caused by C4S (the presence of C4S was found to lower the freezing point of suspension [24, 25]). When the suspensions were re-frozen, new crystals formed (which undoubtedly had different shapes from the original crystals), and therefore disrupted the original pore structures of the collagen-C4S precipitates.

Bending is the major mode of deformation of the heart valve leaflets in vivo [26]. The characteristic anisotropic bending property of the native heart valves can ensure the valves' prompt opening in systole, and prevent sharp reverse curvatures that may cause flexure fatigue in the valve leaflets [27]. Our previous researches examined the mechanical properties of single-composition scaffolds [10], and then utilized these mechanical properties to achieve the bending anisotropy in bi-layer scaffolds [11]. It is now proven that the structurally more advanced tri-layer scaffolds also preserve this desirable feature, in both dry and hydrated statuses.

The anisotropic bending behaviour of the tri-layer scaffold is essentially a result of the fact that a porous scaffold behaves differently (i.e. having different elastic modulus) in compression and tension. When a scaffold is in bending, the effective bending modulus will take into account the compressive modulus of the layer(s) in the compressive region and the tensile modulus of the layer(s) in the tensile region. If the scaffold is then bent to the opposite direction, a different combination of compressive and tensile moduli from the respective regions will be in effect to produce another effective bending modulus. The much higher tensile modulus of the 100%collagen layer is likely to have played the most important role in the complex combinations, and hence has given the scaffold a higher bending modulus in AC direction than in WC direction.

In the self-deflection test on the hydrated scaffold, due to the nature of the test it was not possible to obtain a load-deflection curve and hence not possible to calculate the effective bending modulus of the hydrated scaffold. However, for scaling purposes we can obtain a nominal bending modulus ( $E_{bend.hydr}$ ) of a hydrated scaffold using Eq.3, assuming the hypothetical load-deflection curve is linear. Admittedly, results from the bending tests on dry scaffolds suggest that the load-deflection curves of the hydrated scaffolds should in fact be non-linear, but nonetheless the moduli of different stages on the curves should remain in the same order of magnitude.

$$E_{bend.hydr} = \frac{5ql^4}{384DI} = \frac{5GM_{dry}gl^3}{384DI} \quad \text{Eq.3}$$



In Eq.3,  $G$  is the water uptake ratio of the tri-layer scaffold (determined based on the water uptake ratios of single-composition scaffolds corresponding to respective layers in the tri-layer scaffold, data not shown),  $M_{\text{dry}}$  is the dry mass of the scaffold,  $g$  is the gravitational acceleration,  $l$  is the span distance, and  $I$  is the second moment of area.

Using Eq.3, the deflection values in Table 2 would generate  $E_{\text{bend.hyd}}$  values of  $1.62 \pm 0.23 \text{ kPa}$  in WC direction and  $2.46 \pm 0.18 \text{ kPa}$  in AC direction. These are in agreement with the modulus values of hydrated collagen-GAGs scaffolds reported elsewhere (approximately  $0.2 \text{ kPa}$  in compression and approximately  $2 \text{ kPa}$  in tension) [28].

It has been reported that vascular smooth muscle cells are able to alternate between two phenotypic states: a quiescent contractile state and a proliferative non-contractile state [29-31]. The CDCs in this research may have adopted a similar regime.

Elastin has been found to interact with the cells via a non-integrin signaling pathway and to stimulate actin polymerization [32], which was likely to have caused the contractile phenotype of the CDCs on the single-composition collagen-elastin scaffolds. As a result, these scaffolds demonstrated remarkable volume shrinkage, closing or narrowing the paths for cell migration, which could then explain the smaller stack depth and the higher cell density seen in Fig 9 and Table 4. This was also in agreement with our previous findings that cell proliferation on collagen-elastin scaffolds soon reached saturation due to space constraints [10] and that the collagen-elastin layer exhibited more shrinkage on a bi-layer scaffold after cell culture [11].

However, on the tri-layer scaffolds, the trends seen on the single-composition scaffolds (e.g. stack depth being largest on collagen-C4S scaffolds and smallest on collagen-elastin scaffolds) were just barely followed. The cells distributed relatively evenly on all three layers: cell densities were all between  $3000 \sim 4000 \text{ mm}^{-3}$  and depths of cell migration were all within  $0.3 \sim 0.4 \text{ mm}$ . One possible explanation for these better-mediated cell behaviours was that cell-cell communication or cell movement between adjacent layers (especially that between collagen-C4S layer and collagen-elastin layer) might have evened out the different behaviours of cells.

On the collagen-C4S layer, the cells bound to collagen via integrin receptors [33], and this engagement could activate inter-cellular signal transduction pathways [34]. Moreover, the C4S was able to enhance the metabolic activities of the cells [35] and to promote ECM production (including new collagen and GAGs), which could have further interactions with the other cells [36]. Therefore it was believed that, mediated by the collagen-C4S layer, cells on a tri-layer scaffold

might receive influences from all layers, instead of just one dominating environmental cue as they received on respective single-composition scaffolds. The cell distributions hence equilibrated across the layers.

The relatively crude self-deflection test could be considered a limitation of this work, yet a major potential improvement for the future is, in fact, to characterize the bending properties of the tri-layer scaffolds populated with cells. The seeded cells are likely to increase the modulus of the hydrated scaffolds. As a result, their mechanical properties may be less challenging to measure by conventional methods. However, we could still face problems such as irregular scaffold geometries after cell culture, and more importantly, the difficulties in cell colonization.

It has been reported that there is a critical depth of approximately 500 $\mu$ m for cells migrating into the scaffold in static cell culture [37, 38]. This is due to the formation of a dense layer of cells on the outer surface of scaffold, which acts as a barrier to the diffusion of oxygen and nutrients and hence hinders the pioneering cells from migrating deeper into the scaffold. The CDCs in this study have encountered the same issue. The only exception was the single-composition collagen-C4S scaffold, on which the cells reached a slightly larger depth of 620 $\mu$ m, probably thanks to the non-contractile phenotype mentioned above and the highly hydrophilic C4S. Therefore, in order to achieve complete cell colonization on a tri-layer scaffold that is sufficiently sized for mechanical tests, we may require alternative approaches such as dynamic seeding with bioreactors to facilitate cell migration in the future.

## 5. Conclusion

The tri-layer scaffold produced in this study, to the authors' knowledge, is one of the few artificially designed scaffolds with layered structures and natural polymer compositions relatively similar to those of native heart valves. It is structurally more sophisticated than the existent single-layer scaffolds [9, 39], and also has better controllability and reproducibility compared with the decellularized layered scaffolds [40-42]. The tri-layer scaffold exhibits desirable bending anisotropy in the dry and hydrated statuses. Preliminary results of seeding CDCs on the tri-layer scaffolds have shown satisfactory cell-scaffold interactions, which bode well for utilizing the differentiation capabilities of CDCs in future TEHVs.

## **Acknowledgement**

This study was funded by China Scholarship Council-University of Oxford Scholarship, and by a British Heart Foundation Studentship. The authors would like to acknowledge Prof. Chris Grovenor and Prof. Kieran Clarke for providing the laboratory facilities. Dr. Shaoyang Yeh and Prof. Zhanfeng Cui are thanked for assistance on the multi-photon microscopy.

## References

1. Thom, T., et al., Heart disease and stroke statistics - 2006 Update: A report from the American Heart Association Statistics Committee and Stroke Statistics Subcommittee. *Circulation*, 2006. 113(6): p. e85-e151.
2. Mol, A., et al., Tissue engineering of heart valves: advances and current challenges. *Expert Review of Medical Devices*, 2009. 6(3): p. 259-275.
3. Dohmen, P.M. and W. Konertz, Tissue-engineered heart valve scaffolds. *Annals of Thoracic and Cardiovascular Surgery*, 2009. 15(6): p. 362-367.
4. Breuer, C.K., et al., Application of tissue-engineering principles toward the development of a semilunar heart valve substitute. *Tissue Engineering*, 2004. 10(11-12): p. 1725-1736.
5. Brody, S. and A. Pandit, Approaches to heart valve tissue engineering scaffold design. *Journal of Biomedical Materials Research Part B: Applied Biomaterials*, 2007. 83(1): p. 16-43.
6. Masoumi, N., et al., Tri-layered elastomeric scaffolds for engineering heart valve leaflets. *Biomaterials*, 2014. 35(27): p. 7774-7785.
7. Hoerstrup, S.P., et al., Functional living trileaflet heart valves grown in vitro. *Circulation*, 2000. 102(19): p. III44-III49.
8. Sodian, R., et al., Early in vivo experience with tissue-engineered trileaflet heart valves. *Circulation*, 2000. 102(suppl 3): p. Iii-22-Iii-29.
9. Flanagan, T.C., et al., A collagen-glycosaminoglycan co-culture model for heart valve tissue engineering applications. *Biomaterials*, 2006. 27(10): p. 2233-2246.
10. Chen, Q., et al., Collagen-based scaffolds for potential application of heart valve tissue engineering. *Journal of Tissue Science and Engineering*, 2012. S11: 003.
11. Chen, Q., et al., Bio-mechanical properties of novel bi-layer collagen-elastin scaffolds for heart valve tissue engineering. *Procedia Engineering*, 2013. 59(0): p. 247-254.
12. Sacks, M.S. and A.P. Yoganathan, Heart valve function: A biomechanical perspective. *Philosophical Transactions of the Royal Society B: Biological Sciences*, 2007. 362(1484): p. 1369-1391.
13. Schmidt, D. and S.P. Hoerstrup, Tissue engineered heart valves based on human cells. *Swiss Medical Weekly*, 2006. 136(39-40): p. 618-623.

14. Smith, R.R., et al., Regenerative potential of cardiosphere-derived cells expanded from percutaneous endomyocardial biopsy specimens. *Circulation*, 2007. 115(7): p. 896-908.
15. Friess, W., Collagen - biomaterial for drug delivery. *European Journal of Pharmaceutics and Biopharmaceutics*, 1998. 45(2): p. 113-136.
16. Gustavson, K.H., The chemistry and reactivity of collagen. New York: Academic Press; 1956: 33.
17. Yannas, I.V., Tissue regeneration by use of collagen-glycosaminoglycan copolymers. *Clinical Materials*, 1992. 9(3-4): p. 179-187.
18. Messina, E., et al., Isolation and Expansion of Adult Cardiac Stem Cells From Human and Murine Heart. *Circulation Research*, 2004. 95(9): p. 911-921.
19. Tan, J.-J., et al., Isolation and Expansion of Cardiosphere-Derived Stem Cells. *Current Protocols in Stem Cell Biology*, 2007. 16(1): p. 2C.3.1-2C.3.12.
20. Carr, C.A., et al., Cardiosphere-Derived Cells Improve Function in the Infarcted Rat Heart for at Least 16 Weeks - an MRI Study. *PLoS ONE*, 2011. 6(10): p. e25669.
21. Zipfel, W.R., R.M. Williams, and W.W. Webb, Nonlinear magic: multiphoton microscopy in the biosciences. *Nature biotechnology*, 2003. 21(11): p. 1368-1376.
22. Zipfel, W.R., et al., Live tissue intrinsic emission microscopy using multiphoton-excited native fluorescence and second harmonic generation. *Proceedings of the National Academy of Sciences*, 2003. 100(12): p. 7075-7080.
23. Cui, Z.F., et al., Application of multiple parallel perfused microbioreactors and three-dimensional stem cell culture for toxicity testing. *Toxicology in Vitro*, 2007. 21(7): p. 1318-1324.
24. Atkins, E., Conformation in polysacchrides and complex carbohydrates. *Journal of Biosciences*, 1985. 8(1-2): p. 375-387.
25. Haugh, M.G., C.M. Murphy, and F.J. O'Brien, Novel Freeze-Drying Methods to Produce a Range of Collagen-Glycosaminoglycan Scaffolds with Tailored Mean Pore Sizes. *Tissue Engineering Part C-Methods*, 2009. 16(5): p. 887-894.
26. Merryman, W., et al., The effects of cellular contraction on aortic valve leaflet flexural stiffness. *Journal of Biomechanics*, 2006. 39(1): p. 88-96.

27. Jiang, H., et al., Design and manufacture of a polyvinyl alcohol (PVA) cryogel tri-leaflet heart valve prosthesis. *Medical Engineering & Physics*, 2004. 26(4): p. 269-277.
28. Harley, B.A., et al., Mechanical characterization of collagen-glycosaminoglycan scaffolds. *Acta Biomaterialia*, 2007. 3(4): p. 463-474.
29. Raines, E.W. and R. Ross, Smooth-muscle cells and the pathogenesis of the lesion of atherosclerosis. *British Heart Journal*, 1993. 69(1): p. S30-S37.
30. Owens, G.K., Molecular control of vascular smooth muscle cell differentiation. *Acta Physiologica Scandinavica*, 1998. 164(4): p. 623-635.
31. Thyberg, J., Phenotypic modulation of smooth muscle cells during formation of neointimal thickenings following vascular injury. *Histology and Histopathology*, 1998. 13(3): p. 871-891.
32. Karnik, S.K., et al., A critical role for elastin signaling in vascular morphogenesis and disease. *Development*, 2003. 130(2): p. 411-423.
33. Tuckwell, D. and M. Humphries, Integrin-collagen binding. *Seminars in Cell & Developmental Biology*, 1996. 7(5): p. 649-657.
34. Gille, J. and R.A. Swerlick, Integrins: Role in Cell Adhesion and Communication. *Annals of the New York Academy of Sciences*, 1996. 797(1): p. 93-106.
35. Uygun, B.E., S.E. Stojish, and H.W. Matthew, Effects of immobilized glycosaminoglycans on the proliferation and differentiation of mesenchymal stem cells. *Tissue engineering. Part A*, 2009. 15(11): p. 3499-3512.
36. Chen, Y.-L., et al., Co-conjugating chondroitin-6-sulfate/dermatan sulfate to chitosan scaffold alters chondrocyte gene expression and signaling profiles. *Biotechnology and Bioengineering*, 2008. 101(4): p. 821-830.
37. Lu, H., et al., Cartilage tissue engineering using funnel-like collagen sponges prepared with embossing ice particulate templates. *Biomaterials*, 2010. 31(22): p. 5825-5835.
38. Sachlos, E. and J.T. Czernuszka, Making tissue engineering scaffolds work. Review: the application of solid freeform fabrication technology to the production of tissue engineering scaffolds. *European cells & materials*, 2003. 5: p. 29-39; discussion 39-40.
39. Colazzo, F., et al., Extracellular matrix production by adipose-derived stem cells: Implications for heart valve tissue engineering. *Biomaterials*, 2010. 32(1): p. 119-127.

40. Tedder, M.E., et al., Assembly and Testing of Stem Cell-Seeded Layered Collagen Constructs for Heart Valve Tissue Engineering. *Tissue Engineering Part A*, 2011. 17(1-2): p. 25-36.
41. De Cock, L.J., et al., Layer-by-Layer Incorporation of Growth Factors in Decellularized Aortic Heart Valve Leaflets. *Biomacromolecules*, 2010. 11(4): p. 1002-1008.
42. Elkins, R.C., et al., Decellularized human valve allografts. *Annals of Thoracic Surgery*, 2001. 71(5): p. S428-S432.

**Table 1. Effective bending moduli for the first and second bending stages of the tri-layer scaffolds. <sup>a</sup> denotes significant difference ( $p<0.05$ ) in effective bending modulus between WC and AC directions.**

	WC	AC
$E_{\text{bend1}}$ (kPa)	$54.9 \pm 5.2$	$50.8 \pm 4.9$
$E_{\text{bend2}}$ (kPa)	$13.4 \pm 2.1^a$	$30.0 \pm 0.9^a$

**Table 2. Deflections of hydrated tri-layer scaffolds. <sup>a</sup> denotes significant difference ( $p<0.05$ ) in deflection between WC and AC directions.**

	D (mm)
WC	$2.93 \pm 0.23^a$
AC	$2.27 \pm 0.07^a$

**Table 3. Shrinkage of single-composition scaffolds after 7 days' cell culture, expressed as percentage of area reduction. <sup>a</sup> denotes significant difference ( $p<0.05$ ) between groups.**

Scaffold Composition	Shrinkage (%)
Collagen	$24.4 \pm 8.5$
Collagen-Elastin	$48.5 \pm 2.6^a$
Collagen-C4S	$12.7 \pm 4.2$



**Table 4. Summary of information from the MPM micrographs of single-composition scaffolds.**

	Collagen	Collagen-C4S	Collagen-Elastin
Stack depth (mm)	0.445	0.620	0.169
Stack volume (mm <sup>3</sup> )	0.0313	0.0495	0.0135
Number of cells in stack	45	69	114
Cell density (mm <sup>-3</sup> )	1438	1393	8444

**Table 5. Summary of information from the MPM micrograph of tri-layer scaffold.**

	Collagen layer	Collagen-C4S layer	Collagen-Elasti n layer
Stack depth (mm)	0.337	0.405	0.315
Stack volume (mm <sup>3</sup> )	0.0388	0.0465	0.0362
Number of cells in stack	150	152	134
Cell density (mm <sup>-3</sup> )	3869	3268	3704

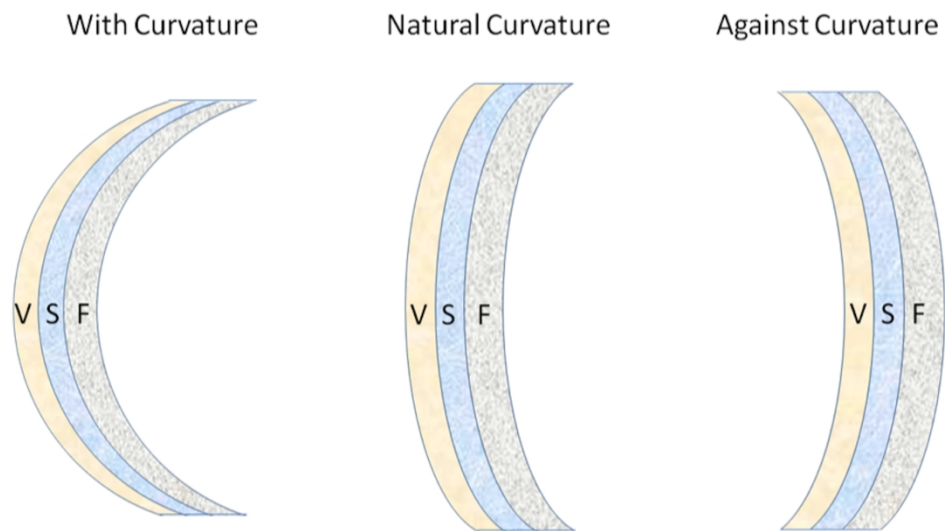


Fig 1. Schematic graph of the bending anisotropy of native heart valve. V, S and F stand for ventricularis, spongiosa and fibrosa, respectively. [12]

191x103mm (300 x 300 DPI)

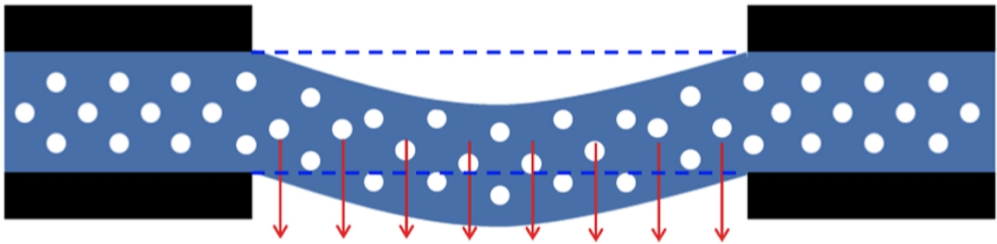


Fig 2. Schematic graph of self-deflection test on hydrated scaffold.  
187x47mm (300 x 300 DPI)

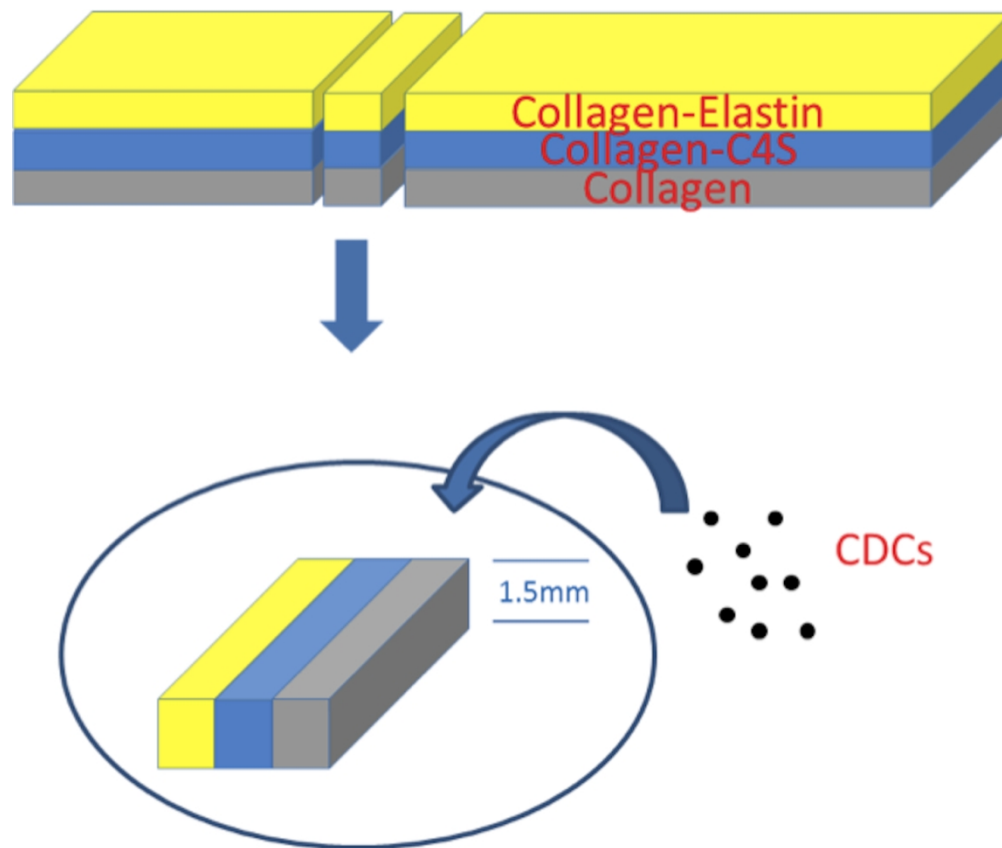


Fig 3. Schematic graph of seeding CDCs onto the tri-layer scaffold. The yellow, blue, and grey layers represent the collagen-elastin, collagen-C4S, and collagen layers respectively. CDCs are seeded onto a section of the original tri-layer scaffold for culturing.

124x104mm (300 x 300 DPI)

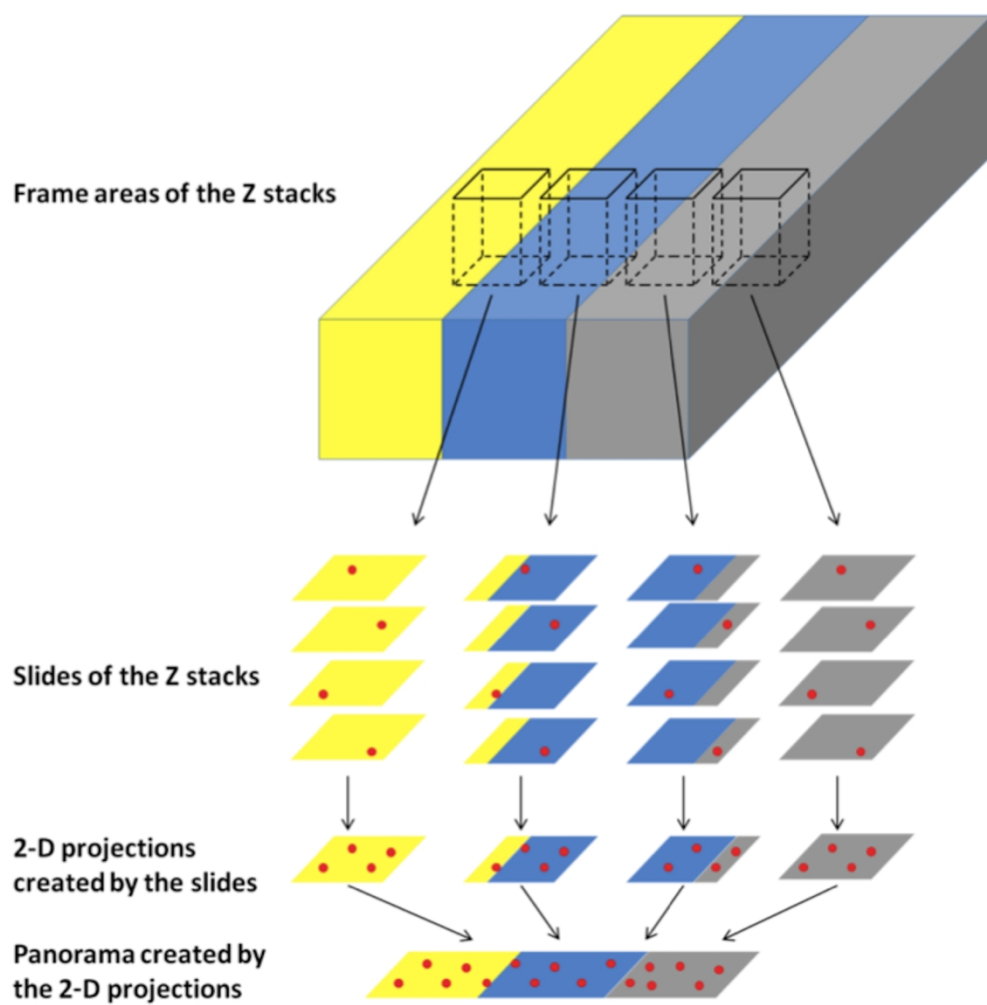


Fig 4. Schematic graph of the procedure of taking MPM images of tri-layer scaffold. A Z stack consisting of multiple slides is taken, and subsequently reconstructed into a 2-D image. Multiple Z stacks are taken across the scaffold and correspondent 2-D images are formed. All of the 2-D images are then stitched to generate a panorama.

150x150mm (300 x 300 DPI)

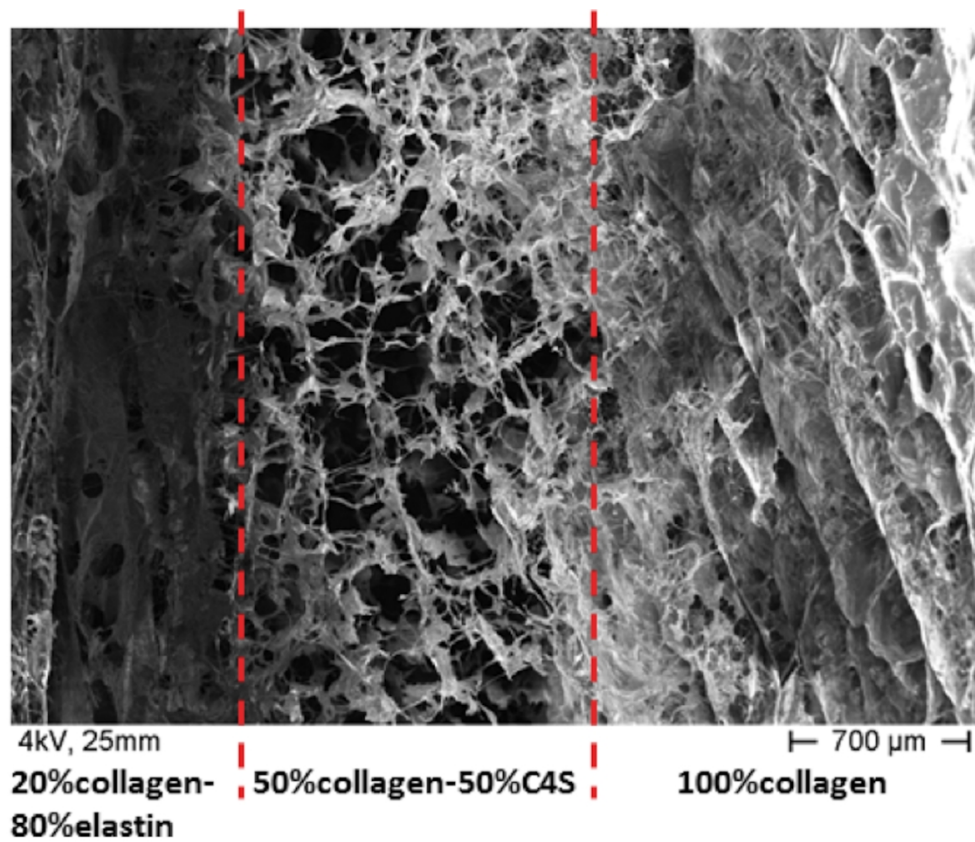


Fig 5. SEM micrograph of cross-section of the tri-layer scaffold. Dashed lines indicate interfaces between layers.

145x125mm (300 x 300 DPI)

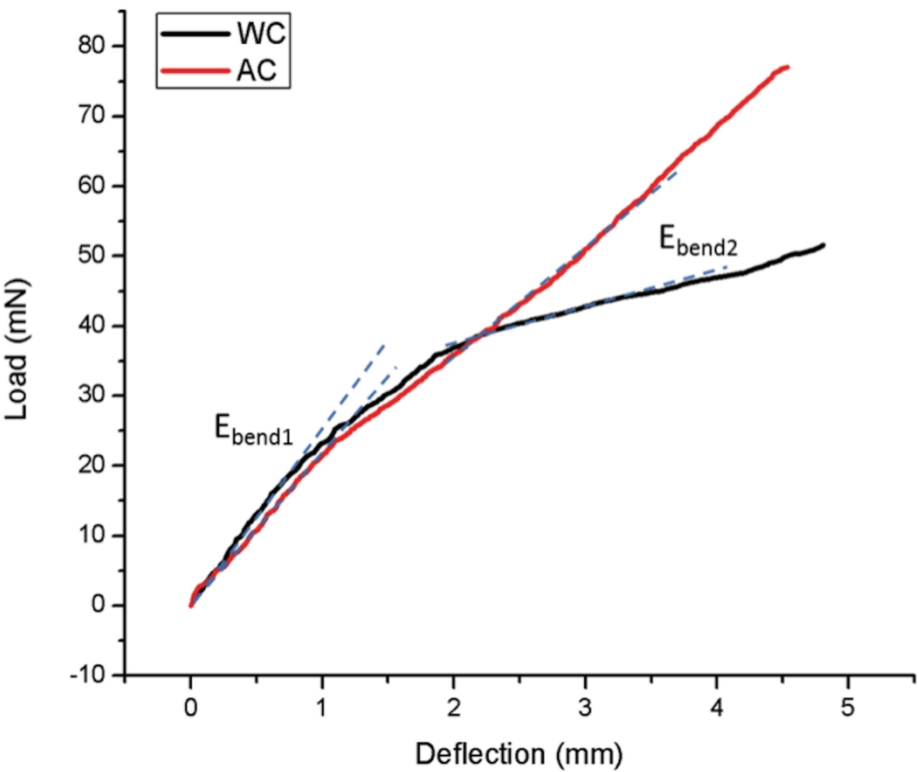


Fig 6. Representative load-deflection curves of tri-layer scaffold bent in WC and AC directions.

171x139mm (300 x 300 DPI)

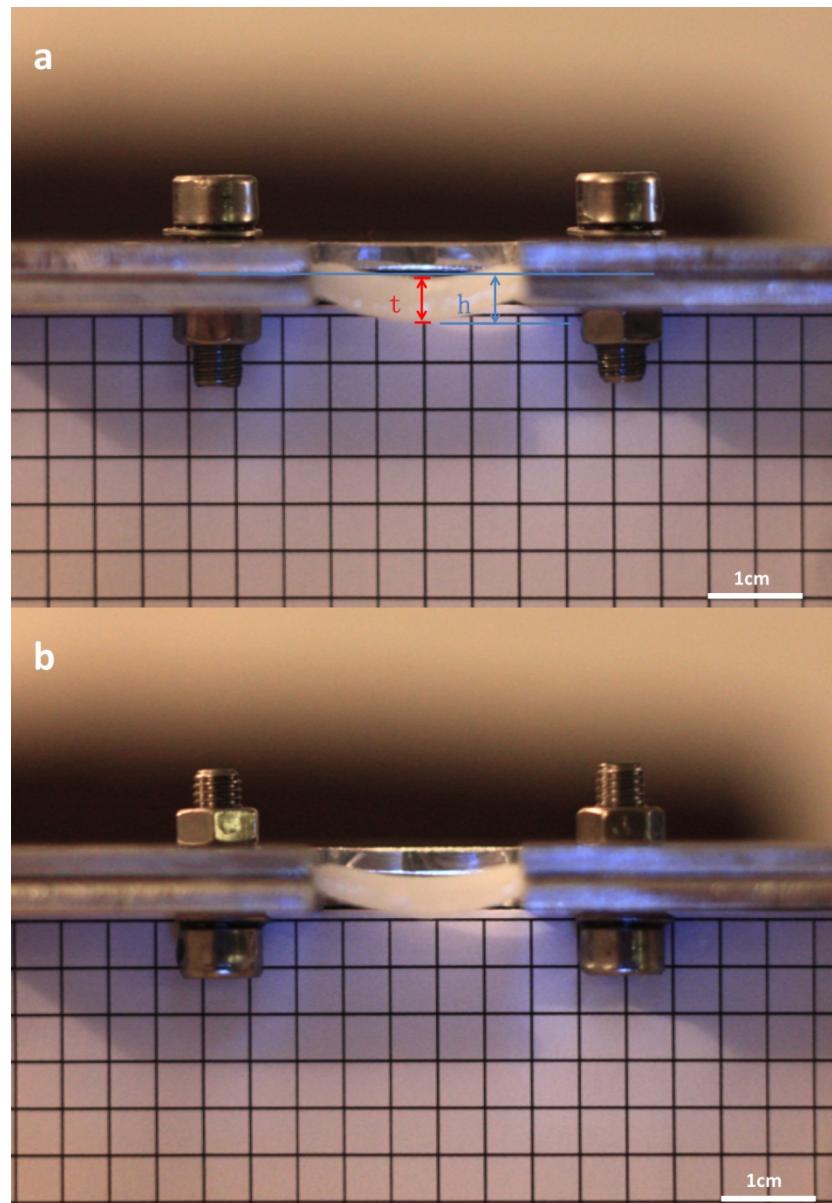


Fig 7. Images of self-deflection tests on a hydrated tri-layer scaffold in (a) WC and (b) AC directions. A grid is used to assist measurements of deflections. The grid units are 5×5mm<sup>2</sup> in size.



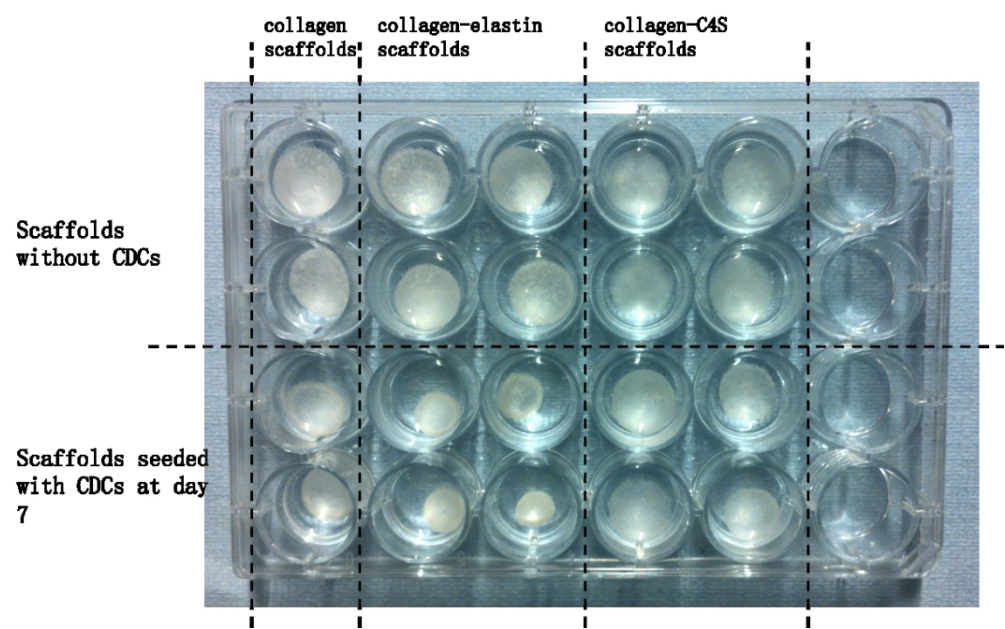


Fig 8. Picture of single-composition scaffolds before and after cell culture. Various degrees of scaffold shrinkage are observed and measured.

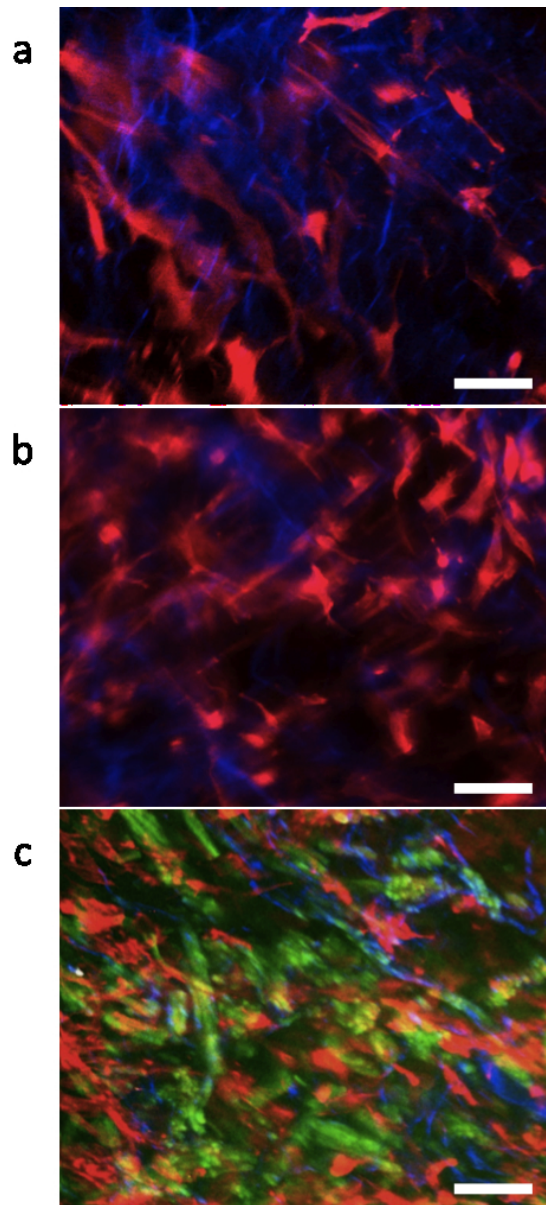


Fig 9. MPM micrographs of CDCs on (a) Collagen scaffold, (b) Collagen-C4S scaffold, and (c) Collagen-Elastin scaffold. Each image is formed by multiple slides in the correspondent Z stack taken on a single-composition scaffold. Scale bar is 50 $\mu$ m.

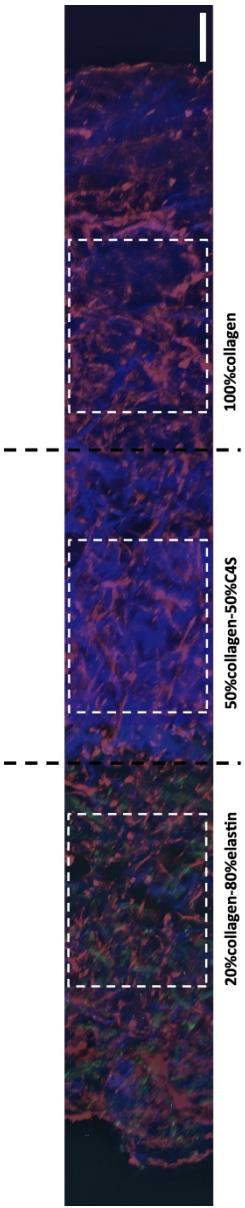


Fig 10. MPM micrograph panorama of CDCs on tri-layer scaffold. Cell density on each layer is measured in the stack indicated by the dashed lines. Scale bar is 100μm.